# Parameter Estimation for a Springpot–Fractional Dashpot Viscoelastic Model: Optimisation and Numerical Laplace Inversion

L. L. Ferrás[1,2(✉)], C. Coelho[3], M. Fernanda P. Costa[2], M. L. Morgado[4,5], and M. Rebelo[6]

[1] CEFT, ALiCE, Faculty of Engineering, University of Porto, 4200-465 Porto, Portugal
lferras@fe.up.pt

[2] Centre of Mathematics (CMAT), University of Minho, 4710-57 Braga, Portugal
mfc@math.uminho.pt

[3] Institute for Artificial Intelligence, Helmut Schmidt University, 22043 Hamburg, Germany
cecilia.coelho@hsu-hh.de

[4] Departamento de Matemática, Universidade de Trás-os-Montes e Alto Douro, UTAD, 5001-801 Vila Real, Portugal
luisam@utad.pt

[5] Center for Computational and Stochastic Mathematics, Instituto Superior Técnico, Lisbon, Portugal

[6] Center for Mathematics and Applications (NOVA Math) and Department of Mathematics, NOVA School of Science and Technology (NOVA FCT), Campus de Caparica, Caparica2829-516, Portugal
msjr@fct.unl.pt

**Abstract.** This work addresses the parameter estimation of a fractional viscoelastic model comprising a springpot and a fractional dashpot arranged in series. Key features of the model, including the relaxation modulus, are formulated in the Laplace domain and subsequently evaluated in the time domain through numerical inversion using the Talbot method.

A two-step optimisation strategy is adopted to identify the model parameters efficiently. In the first stage, frequency-domain data, namely the storage and loss moduli, are used to estimate an initial set of parameters. In the second stage, these preliminary estimates are refined by performing an optimisation that incorporates both frequency-domain data and time-domain data (relaxation modulus).

Since the relaxation modulus is obtained through an inverse Laplace transform and does not admit a closed-form expression in the time domain, a sequential iterative procedure is employed during the second stage. In this approach, the relaxation modulus is first computed numerically using the Talbot method, after which the parameters are updated through optimisation. This process is repeated iteratively until a prescribed tolerance is satisfied.

© The Author(s), under exclusive license to Springer Nature Switzerland AG 2027
O. Gervasi et al. (Eds.): ICCSA 2026 Workshops, LNCS 16763, pp. 285–297, 2027.
https://doi.org/10.1007/978-3-032-30530-5_18

Validation against experimental data obtained for a low-density polyethylene demonstrates that the proposed methodology accurately reproduces both frequency- and time-domain responses, highlighting the effectiveness of fractional models in capturing complex viscoelastic behaviour.

**Keywords:** Optimisation · Viscoelastic models · Rheology · Talbot Method · Springpot · Fractional-Dashpot

## 1 Introduction

The modelling of viscoelastic fluids [1] using fractional elements [3–7,10,15] has proven to be an effective way to capture complex relaxation behaviour with a reduced number of parameters. In this context, the fractional dashpot model introduced by Yao [20] provides a continuous interpolation between viscous and Maxwell-type responses, while retaining a compact mathematical structure. Nevertheless, many complex fluids exhibit a distribution of relaxation mechanisms that cannot be adequately described by a single fractional dashpot and inherent timescales.

To overcome this limitation, we propose an extended configuration consisting of a springpot connected in series with a fractional dashpot [8]. This construction preserves the dissipative nature of the original formulation, while introducing additional flexibility to represent a broader class of material responses. In contrast with classical multimode approaches, which rely on a superposition of many discrete relaxation modes, the present formulation incorporates multiple memory effects through fractional operators, leading to a smoother and more compact representation of the relaxation spectrum.

From a physical perspective, the series arrangement can be interpreted as the interaction of two distinct dissipative mechanisms acting at different temporal scales. This interpretation is consistent with the hierarchical relaxation processes typically observed in polymeric and complex fluids. At the same time, the use

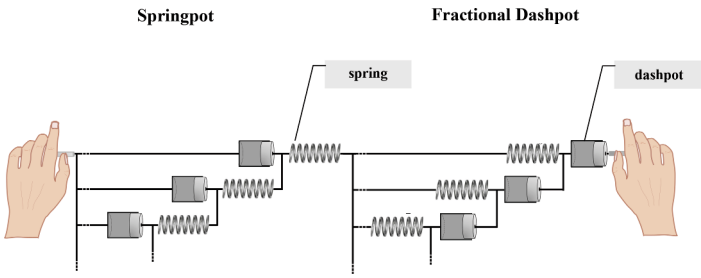


**Fig. 1.** Mechanical analogue consisting of a springpot and a fractional dashpot connected in series. The ladder-type representation associated with the fractional dashpot follows the construction introduced in Yao's model.

of fractional operators ensures a parsimonious description, avoiding the need for a large number of fitting parameters.

We consider a mechanical system composed of a springpot and a fractional dashpot connected in series, as depicted in Fig. 1.

The strain in the springpot element is given by

$$\gamma_1(t) = \frac{1}{\mathbb{V}} D_t^{-\alpha} \sigma(t),$$

where $D_t^{-\alpha}$ denotes the Riemann-Liouville fractional integral [2] of order $\alpha \in (0,1)$.

For the fractional dashpot, the strain rate is expressed as

$$\dot{\gamma}_2(t) = \frac{e^{-t/\lambda}}{g\lambda^\beta} D_t^{1-\beta} \left( e^{t/\lambda} \sigma(t) \right),$$

with $\beta \in (0,1)$, where $D_t^{1-\beta}$ denotes the Caputo fractional derivative of order $(1-\beta)$ [2].

Since the elements are arranged in series, the total strain satisfies

$$\gamma(t) = \gamma_1(t) + \gamma_2(t).$$

Combining the previous expressions leads to the constitutive relation [8],

$$g\lambda^\beta D_t^{1-\alpha} \sigma(t) + \mathbb{V} e^{-t/\lambda} D_t^{1-\beta} \left( e^{t/\lambda} \sigma(t) \right) = \mathbb{V} g \lambda^\beta \dot{\gamma}(t). \tag{1}$$

Here, $g$, $\mathbb{V}$ and $\lambda$ are positive material parameters. $D_t^\mu$ denotes the Caputo fractional derivative of order $\mu \in (0,1)$, defined for a sufficiently smooth function $f$ by,

$$D_t^\mu f(t) = \frac{1}{\Gamma(1-\mu)} \int_0^t (t-\tau)^{-\mu} f'(\tau)\, d\tau, \quad 0 < \mu < 1.$$

The original fractional dashpot model proposed by Yao is recovered as a limiting case of (1) by dividing through by $\mathbb{V}$ and considering the limit $\mathbb{V} \to \infty$.

This work is organised as follows. Section 2 introduces the relevant rheological functions, including the storage and loss moduli and the relaxation modulus. In Sect. 3, the Talbot method is presented, together with the optimisation problems used to estimate the model parameters. Section 4 describes the optimisation strategy adopted to solve these problems, and demonstrates that the optimal parameter values enable the model to reproduce the experimental data with high accuracy while using a smaller number of parameters. Finally, the paper concludes in Sect. 5.

## 2 Rheological Functions

In this section, we present key rheological functions associated with the constitutive model (1), namely the storage modulus, the loss modulus, and the relaxation

modulus. These functions provide essential information about the material's viscoelastic behaviour in both the frequency and time domains.

For parameter estimation, only these three functions are considered. The storage and loss moduli, measured in the frequency domain, are used to characterise the oscillatory response of the material, while the relaxation modulus, measured in the time domain, captures the stress relaxation behaviour. Together, they provide sufficient and complementary information to reliably identify the model parameters and demonstrate the robustness of the proposed fitting methodology.

### 2.1 Storage and Loss Modulus

The storage modulus $G'(\omega)$ and the loss modulus $G''(\omega)$ are obtained from the complex modulus $G^*(\omega)$ by evaluating the Laplace-domain transfer function along the imaginary axis, i.e., $s = i\omega$. They are given by [8]:

$$G'(\omega) = \frac{\mathbb{V} g \lambda^\beta \, \omega \, B(\omega)}{A^2(\omega) + B^2(\omega)},$$
$$G''(\omega) = \frac{\mathbb{V} g \lambda^\beta \, \omega \, A(\omega)}{A^2(\omega) + B^2(\omega)},$$

where the auxiliary functions $A(\omega)$ and $B(\omega)$ correspond to the real and imaginary parts of the denominator, respectively, and are defined as

$$A(\omega) = g\lambda^\beta \omega^{1-\alpha} \cos\left(\frac{(1-\alpha)\pi}{2}\right) + \mathbb{V}\left(\omega^2 + \lambda^{-2}\right)^{\frac{1-\beta}{2}} \cos\big((1-\beta)\phi(\omega)\big),$$
$$B(\omega) = g\lambda^\beta \omega^{1-\alpha} \sin\left(\frac{(1-\alpha)\pi}{2}\right) + \mathbb{V}\left(\omega^2 + \lambda^{-2}\right)^{\frac{1-\beta}{2}} \sin\big((1-\beta)\phi(\omega)\big),$$

with

$$\phi(\omega) = \arctan(\omega\lambda).$$

### 2.2 Relaxation Modulus

The relaxation modulus $G(t)$ is defined through the stress response to a unit step strain. In the Laplace domain, it is given by [8]:

$$\tilde{G}(s) = \frac{\mathbb{V}}{s^{1-\alpha} + a(s+b)^{1-\beta}},$$

where

$$a = \frac{\mathbb{V}}{g\lambda^\beta}, \qquad b = \lambda^{-1},$$

and $s \in \mathbb{C}$ denotes the Laplace variable.

The time-domain relaxation modulus is then obtained via the inverse Laplace transform:

$$G(t) = \mathbb{V}\,\mathcal{L}^{-1}\left\{\frac{1}{s^{1-\alpha} + \dfrac{\mathbb{V}}{g\lambda^{\beta}}\,(s+\lambda^{-1})^{1-\beta}}\right\}(t).$$

## 3 Optimisation Problems and Talbot Method

### 3.1 Numerical Inversion via the Talbot Method

Time-domain rheological functions, such as the relaxation modulus $G(t)$, are obtained as inverse Laplace transforms of their corresponding Laplace-domain expressions. In fractional viscoelastic models, these Laplace-domain expressions typically involve fractional powers of the Laplace variable and special functions, for which closed-form inverse transforms are rarely available. Consequently, reliable and efficient numerical inversion techniques are required to evaluate the time-domain responses.

The inverse Laplace transform of a function $\tilde{f}(s)$ is formally defined by the Bromwich integral

$$f(t) = \frac{1}{2\pi i}\int_{\mathbb{L}} e^{st}\tilde{f}(s)\,ds, \qquad t > 0,$$

where $\mathbb{L}$ denotes a vertical contour in the complex plane, defined by

$$\mathbb{L} = \{s = \gamma + i\omega : \omega \in (-\infty, \infty)\},$$

with $\gamma$ chosen such that all singularities of $\tilde{f}(s)$ lie to the left of the contour. Although this representation is mathematically well-defined, its direct numerical evaluation is challenging due to the oscillatory behaviour of the exponential term $e^{st}$, especially for large values of $|\omega|$. Additionally, the integrand often decays slowly, making standard quadrature methods inefficient and potentially unstable.

To overcome these difficulties, Talbot proposed deforming the Bromwich contour into a more suitable path in the complex plane [13]. The resulting contour, commonly referred to as the Talbot contour, is designed to ensure rapid decay of the exponential term while maintaining analyticity of the integrand. This contour deformation relies on Cauchy's integral theorem, which guarantees that the value of the inverse Laplace transform remains unchanged as long as the deformed contour does not cross any singularities of $\tilde{f}(s)$.

The Talbot contour is typically parameterized as

$$s(\theta) = \frac{N}{t}\,\phi(\theta), \qquad -\pi \le \theta \le \pi,$$

where $\phi(\theta)$ is a suitably chosen complex-valued function that defines the contour shape, and $N$ is the number of quadrature points. A commonly used parameterization is given by

$$\phi(\theta) = a\,\theta\cot(\theta) + ib\,\theta + c,$$

where $a$, $b$, and $c$ are real parameters selected to optimise convergence and numerical stability. This contour bends into the left half-plane, ensuring that the real part of $s(\theta)$ is negative for most values of $\theta$, thereby enforcing exponential decay in $e^{st}$.

After parameterization, the Bromwich integral is transformed into a contour integral in terms of the parameter $\theta$,

$$f(t) = \frac{1}{2\pi i} \int_{-\pi}^{\pi} e^{s(\theta)t} \tilde{f}(s(\theta)) s'(\theta)\, d\theta.$$

This integral is then approximated numerically using the trapezoidal rule, which is particularly effective for periodic integrands. The resulting discrete approximation takes the form

$$f(t) \approx \sum_{k=0}^{N-1} \omega_k\, e^{s_k t} \tilde{f}(s_k),$$

where the quadrature nodes $s_k = s(\theta_k)$ lie on the Talbot contour, with

$$\theta_k = -\pi + \frac{2\pi k}{N}, \qquad k = 0, \ldots, N-1,$$

and the weights $\omega_k$ incorporate both the trapezoidal coefficients and the derivative of the contour parameterization.

One of the key advantages of the Talbot method is its high accuracy with relatively few evaluation points. In practice, accurate results are typically obtained with modest values of $N$, making the method computationally efficient. Furthermore, the Talbot method is particularly well suited for functions arising in fractional calculus, where branch points and fractional powers frequently appear in the Laplace domain.

Another important feature of the Talbot method is its robustness with respect to different time scales. The contour scaling is adapted according to the value of $t$, ensuring stable computations for both short- and long-time responses. This property is especially relevant in viscoelastic modelling, where the material response may span several orders of magnitude in time.

In this work, the Talbot method [13] is therefore employed to compute the inverse Laplace transform of the relaxation modulus $G(t)$. These numerical inversions are performed repeatedly during the optimisation procedure, making computational efficiency essential.

### 3.2 Optimisation Problems

The parameters $\alpha$, $\beta$, $\lambda$, $\mathbb{V}$, and $g$ that define the proposed viscoelastic model are not known a priori and must therefore be estimated from experimental observations. In this work, these parameters are determined by solving optimisation problems that minimise the discrepancy between experimental data and the corresponding model predictions.

Two distinct experimental datasets are considered: (i) storage and loss moduli obtained in the frequency domain, and (ii) relaxation modulus obtained in the time domain. A two-step optimisation strategy is adopted here.

In the first step, the parameters are estimated using the storage and loss moduli data (denoted as *Problem 1*). This will result in the initial set of parameters ($\alpha_0$, $\beta_0$, $\lambda_0$, $\mathbb{V}_0$, and $g_0$) to be used in the second step, where storage, loss and relaxation modulus data are used to obtain the optimal set of parameters (denoted as *Problem 2*).

– *(Problem 1):* The estimation of parameters $\alpha$, $\beta$, $\lambda$, $\mathbb{V}$, and $g$ is formulated as the following nonlinear least-squares optimisation problem:

$$\min_{\lambda,g,\alpha,\beta,\mathbb{V}\in\mathbb{R}} E_{G',G''}(\lambda,g,\alpha,\beta,\mathbb{V}) = \sum_{l=1}^{N_{G'G''}} \left( \left[ \frac{\hat{G}'(\omega)_l}{G'_l} - 1 \right]^2 + \left[ \frac{\hat{G}''(\omega)_l}{G''_l} - 1 \right]^2 \right)$$
$$\text{subject to} : \lambda > 0, g > 0, \mathbb{V} > 0,$$
$$\alpha, \beta \in (0,1).$$

Here, $N_{G'G''}$ denotes the total number of experimental observations available for the storage modulus $G'_l$ and the loss modulus $G''_l$. The quantities $\hat{G}'(\omega)_l$ and $\hat{G}''(\omega)_l$ correspond to the values predicted by the model, evaluated at the angular frequency $\omega_l$.

To solve *Problem 1*, the optimisation procedure is performed using the IPOPT solver, available through the NEOS server (http://neos.mcs.anl.gov/neos/solvers). The IPOPT (Interior Point OPTimizer) is designed for large-scale nonlinear programming problems and is based on an interior-point framework combined with a line-search filter strategy. This approach incorporates barrier methods together with filter-based acceptance criteria, allowing efficient handling of nonlinear constraints and improving convergence properties. Further details regarding the algorithmic structure and theoretical foundations can be found in [14,16–19].

For comparison purposes, the Generalized Reduced Gradient (GRG) nonlinear solver was also considered. This method optimises continuous parameters by iteratively computing descent directions that reduce the objective function. Consequently, the algorithm adjusts the model parameters so that the resulting smooth function provides a close agreement with the experimental data.

– *(Problem 2):* After obtaining the initial estimates $\alpha_0$, $\beta_0$, $\lambda_0$, $\mathbb{V}_0$, and $g_0$, we proceeded by solving the following optimisation problem:

$$\min_{\lambda,g,\alpha,\beta,\mathbb{V}\in\mathbb{R}} E_{G',G'',G}(\lambda,g,\alpha,\beta,\mathbb{V}) = \sum_{l=1}^{N_{G'G''}} \left( \left[ \frac{\hat{G}'(\omega)_l}{G'_l} - 1 \right]^2 + \left[ \frac{\hat{G}''(\omega)_l}{G''_l} - 1 \right]^2 \right)$$
$$+ \sum_{l=1}^{N_G} \left[ \frac{\hat{G}(t)_l}{G_l} - 1 \right]^2$$
$$\text{subject to} : \lambda > 0, g > 0, \mathbb{V} > 0,$$
$$\alpha, \beta \in (0,1).$$

In this formulation, $N_G$ denotes the number of experimental data points for the relaxation modulus $G_l$, while $\hat{G}(t)_l$ represents the model prediction evaluated at time $t_l$.

It is important to note that the evaluation of $\hat{G}(t)$ requires the computation of an inverse Laplace transform. Therefore, we adopt a sequential solution strategy. In this approach, the optimisation algorithm operates only in the parameter space, while the inverse Laplace transform is computed separately at each iteration.

More specifically, for each candidate set of parameters, the inverse Laplace transform is computed using the Talbot method, followed by the evaluation of the objective function. This sequential procedure results in a bound-constrained optimisation problem that can be efficiently handled using standard nonlinear optimisation techniques.

The overall workflow of the sequential approach adopted for solving *Problem 2* is illustrated in Fig. 2.

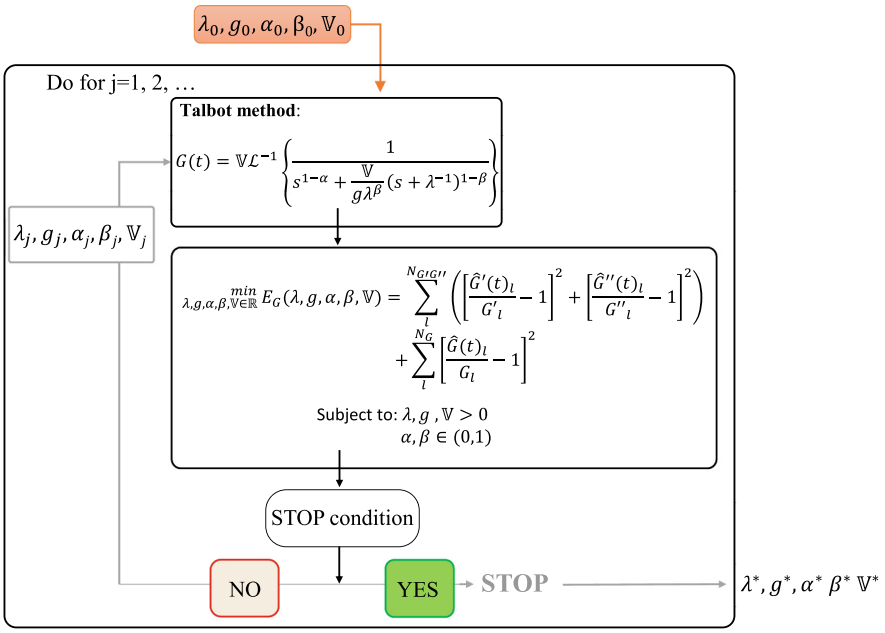


**Fig. 2.** Sequential algorithm used to solve *Problem 2*.

## 4 Fit to Data

We now present a fit to experimental data reported in [9] for the storage and loss modulus of a low-density polyethylene. The data were collected at different temperatures and shifted using the Williams–Landel–Ferry (WLF) equation

[11] to obtain a master curve. In addition, we consider experimental measurements of the relaxation modulus as a function of time for the same low-density polyethylene at 150°C.

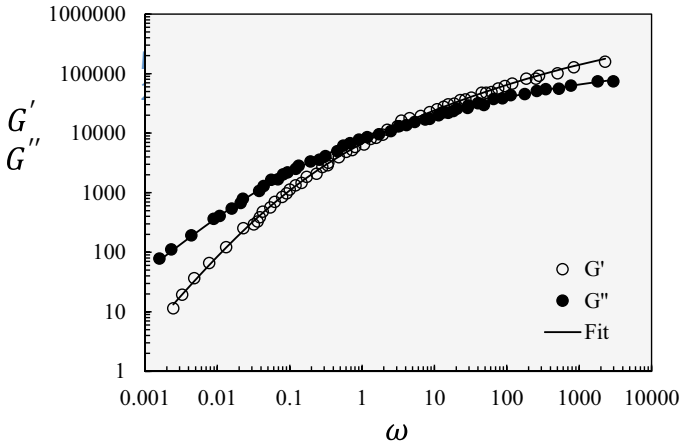


**Fig. 3.** Fit to experimental data reported in [9] for the storage and loss moduli (Pa) of a low-density polyethylene as functions of the angular frequency $\omega$ (rad/s).

The optimisation problem *Problem 1* was implemented using AMPL without presolve.

The optimisation problem was then solved using the IPOPT solver with default parameter settings. The solver was initialised with a set of starting values for the model parameters. After solving *Problem 1*, the following parameter estimates were obtained and subsequently used as initial guesses for *Problem 2*: $\alpha_0 = 0.51$, $\beta_0 = 0.15$, $\lambda_0 = 0.6$, $\mathbb{V}_0 = 14000$, and $g_0 = 80000$, yielding an objective function value of $E^*_{G',G''} = 0.5084$.

This optimal solution was achieved after 16 objective function evaluations, together with 16 evaluations of the objective gradient, 16 evaluations of the inequality constraints, 16 evaluations of the constraint Jacobian, and 16 evaluations of the Lagrangian Hessian. The total computational time reported by IPOPT (excluding function evaluations) was 0.05 CPU seconds, while the time spent on nonlinear programming function evaluations was 0.07 CPU seconds. All computations were carried out using the free NEOS cloud computing service.

To determine the final parameter values, *Problem 2* was solved using the sequential procedure illustrated in Fig. 2. This approach was implemented in Matlab®, where the inverse Laplace transform required for the evaluation of the relaxation modulus was computed numerically (the number of terms to sum for each $t$ was 64 [12]) for each iteration.

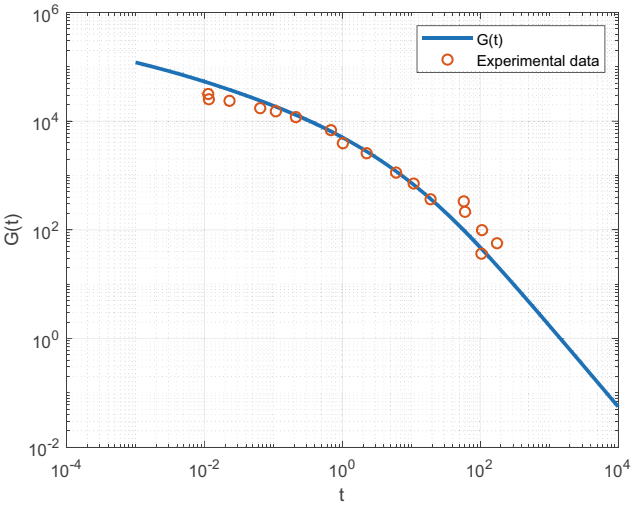


**Fig. 4.** Fit to experimental data reported in [9] for the relaxation modulus $G(t)$ (Pa) of a low-density polyethylene as a function of time $t$ (s).

The optimisation was performed using the *fmincon* function with the interior-point algorithm. A stopping criterion based on a tolerance of $1 \times 10^{-10}$ was adopted, while all remaining solver parameters were kept at their default values.

The optimisation procedure converged after 10 iterations, leading to the following optimal parameter values: $\alpha_0 = 0.4984$, $\beta_0 = 0.1513$, $\lambda_0 = 0.5678$, $\mathbb{V}_0 = 13084.8022$, and $g_0 = 90309.8388$.

The resulting global error was $E_{G',G'',G} = 0.6126$. This relatively small error indicates that the proposed model provides an accurate representation of the experimental data. In particular, a very good agreement was obtained for both the storage and loss moduli (Fig. 3) and the relaxation modulus (Fig. 4).

## 5 Conclusions

In this work, a fractional viscoelastic model composed of a springpot connected in series with a fractional dashpot was proposed, together with a systematic strategy for parameter identification based on experimental rheological data. Fractional models of this type offer a flexible and compact framework for representing complex viscoelastic behaviour using a limited number of physically meaningful parameters. In particular, the proposed configuration is capable of capturing both short- and long-time memory effects, which are frequently observed in polymeric materials and are often difficult to reproduce using classical integer-order constitutive models.

The model parameters were identified using experimental data obtained in both the frequency and time domains, namely the storage modulus, the loss modulus, and the relaxation modulus. These complementary datasets provide a

good characterisation of the viscoelastic response and enable a more reliable estimation of the model parameters. To enhance both robustness and computational efficiency, a two-step optimisation strategy was adopted.

In the first stage, parameter estimation was performed by fitting the storage and loss modulus data. The corresponding optimisation problem was formulated as a nonlinear least-squares problem, in which the objective function measures the discrepancy between experimental observations and model predictions over a range of angular frequencies. This problem was solved using the IPOPT solver, which is well suited for nonlinear optimisation problems with bound constraints. The resulting parameter estimates were stable and physically meaningful, and were subsequently used as initial guesses for the second stage.

In the second stage, the optimisation procedure incorporated both frequency-domain data and time-domain data through the relaxation modulus. Since the relaxation modulus is obtained by numerically inverting Laplace-domain expressions, the resulting optimisation problem becomes computationally more demanding. To address this difficulty, a sequential approach was adopted, whereby the numerical inversion using the Talbot method and the optimisation procedure were performed iteratively until convergence was achieved.

The results demonstrate that the proposed fractional model provides an excellent agreement with the experimental data in both the frequency and time domains. In particular, the model accurately reproduces the storage and loss moduli over the entire frequency range considered, as well as the relaxation modulus across the time interval analysed. These findings confirm the capability of the springpot–fractional dashpot configuration to capture complex viscoelastic behaviour, including power-law responses and long-memory effects characteristic of fractional-order models.

Moreover, the proposed optimisation strategy proved to be robust and computationally efficient, allowing reliable parameter estimation even when numerical inversion of Laplace-domain expressions is required.

A limitation of the present work is that the parameter identification and validation procedures were carried out using experimental data corresponding only to a single material, namely low-density polyethylene. Although the obtained results demonstrate the suitability of the proposed fractional viscoelastic model for this polymer, the general applicability of the model to other classes of viscoelastic materials remains to be investigated. In particular, materials exhibiting different rheological characteristics, such as highly filled polymers, biological tissues, elastomers, or composite materials, may require different fractional structures or additional constitutive elements to accurately capture their behaviour. Furthermore, the identification procedure considered only three types of experimental data: the storage modulus, the loss modulus, and the relaxation modulus. While these quantities provide important information regarding the linear viscoelastic response, other experimental measurements, such as creep compliance, stress–strain, or nonlinear rheological tests, were not included and could provide additional validation of the model and its predictive capabilities.

Future work may therefore focus on extending the proposed methodology to a broader range of viscoelastic materials and experimental conditions. In par-

ticular, it would be of interest to investigate the performance of the model for materials exhibiting nonlinear or temperature-dependent behaviour, as well as to study the robustness of the parameter identification procedure under noisy or incomplete experimental data. Additional developments may also include the incorporation of other rheological tests, such as creep and dynamic loading experiments, into the optimisation framework in order to improve parameter identifiability and model reliability. From a computational perspective, alternative numerical inversion techniques and more advanced optimisation strategies could be explored to further reduce computational cost and improve convergence properties. Finally, the extension of the proposed fractional framework to multidimensional constitutive models and its implementation in numerical simulation methods, would constitute an important step toward practical engineering applications.

**Acknowledgments.** We thank the support of the High-Performance Computing Center at the University of Évora funded by FCT I.P. under the project "OptXAI: Constrained optimisation in NNs for Explainable, Ethical and Greener AI", reference 2024.00191.CPCA.A1, platform Vision. This work was financially supported by national funds through the FCT/MCTES (PIDDAC) under the project 2022.06672.PTDC—iMAD (Improving the Modelling of Anomalous Diffusion and Viscoelasticity: solutions to industrial problems), DOI 10.54499/2022.06672.PTDC (https://doi.org/ 10.54499/ 2022.06672.PTDC); and by the project UID/00013/2025 (https://doi.org/10.54499/UID/00013/2025) (CMAT). It was also financially supported by Fundação "la Caixa"|BPI and FCT through project PL24-00057: "Inteligência Artificial na Otimização da Rega para Olivais Resilientes às Alterações Climáticas". C. Coelho would like to thank the KIBIDZ project funded by dtec.bw-Digitalization and Technology Research Center of the Bundeswehr; dtec.bw is funded by the European Union-NextGenerationEU.

M.L. Morgado acknowledges funding by FCT - Fundação para a Ciência e a Tecnologia, through the project https://doi.org/10.54499/UID/04621/2025.

L.L. Ferrás acknowledges FCT - Fundação para a Ciência e a Tecnologia, for financial support through FCT/MECI: CEFT, UID/00532/2025 (https://doi.org/10.54499/UID/ 00532/2025) and UID/PRR/ 00532/2025 (https://doi.org/10.54499/UID/PRR/ 00532/2025) and ALiCE, LA/P/0045/2020 (https:// doi.org/10.54499/LA/P /0045 /2020).

M. Rebelo acknowledges FCT – Fundação para a Ciência e a Tecnologia, I.P., under the scope of the projects UID/00297/2025 (https://doi.org/10.54499/UID/00297/ 2025) and UID/PRR/00297/2025 (https://doi.org/10.54499/UID/PRR/00297/2025) (Center for Mathematics and Applications – NOVA Math).

## References

1. Bird, R.B., Armstrong, R.C., Hassager, O.: Dynamics of Polymeric Liquids. Vol. 1: Fluid Mechanics. A Wiley-Interscience Publication, John Wiley & Sons (1987)
2. Diethelm, K.: The Analysis of Fractional Differential Equations. Lecture Notes in Mathematics, vol. 2004. Springer, Berlin, Heidelberg (2010). https://doi.org/10.1007/978-3-642-14574-2

3. Ferrás, L.L., et al.: Theoretical and numerical analysis of unsteady fractional viscoelastic flows in simple geometries. Comput. Fluids **174**, 14–33 (2018)
4. Ferrás, L.L., Luísa, M., Rebelo, M., Mckinley, G.H., Afonso, A.: A generalized phan-thien – tanner model. J. Nonnewton. Fluid Mech. **269**, 88–99 (2019)
5. Ferrás, L.L., Morgado, M.L., Rebelo, M.: A numerical method for the transient couette flow of a distributed-order viscoelastic fluid. In: Gervasi, O., et al. (eds.) Computational Science and Its Applications – ICCSA 2021, Lecture Notes in Computer Science, vol. 12952. Springer, Cham (2021)
6. Ferrás, L.L., Morgado, M.L., Rebelo, M.: A generalised distributed-order maxwell model. Math. Methods Appl. Sci. **46**(1), 368–387 (2023)
7. Ferrás, L.L., Rebelo, M., Morgado, M.L.: The role of the weight function in the generalised distributed-order maxwell model: the case of a distributed-springpot and a dashpot. Appl. Math. Model. **122**, 844–860 (2023)
8. Henriques, R.O., Ferrás, L.L., Rebelo, M., Morgado, L.M.: Mathematical analysis of a novel linear fractional viscoelastic model exhibiting fluid-like behaviour (2026), manuscript submitted for publication
9. Laun, H.M.: Description of the non-linear shear behaviour of a low density polyethylene melt by means of an experimentally determined strain dependent memory function. Rheol. Acta **17**(1), 1–15 (1978)
10. Leiva, R.T., Ferrás, L.L., Castelo, A., et al.: A generalisation of the integral maxwell model: the GK-BKZ model–frame invariance and analytical solutions. Meccanica **59**, 363–384 (2024)
11. Macosko, C.W.: Rheology: Principles, Measurements, and Applications. Wiley-VCH, New York (1994)
12. McClure, T.: Numerical inverse laplace transform. https://www.mathworks.com/matlabcentral/fileexchange/39035-numerical-inverse-laplace-transform (2026). Retrieved: 19 Mar 2026
13. Murli, A., Rizzardi, M.: Algorithm 682: Talbot's method for the laplace inversion problem. ACM Trans. Math. Softw. **16**(2), 158–168 (1990)
14. Nocedal, J., Wächter, A., Waltz, R.A.: Adaptive barrier strategies for nonlinear interior methods. SIAM J. Optim. **19**(4), 1674–1693 (2009)
15. Schiessel, H., Metzler, R., Blumen, A., Nonnenmacher, T.F.: Generalized viscoelastic models: their fractional equations with solutions. J. Phys. A: Math. Gen. **28**, 6567–6584 (1995)
16. Wächter, A.: An Interior Point Algorithm for Large-Scale Nonlinear Optimization with Applications in Process Engineering. Ph.D. thesis, Carnegie Mellon University, Pittsburgh, PA, USA (2002)
17. Wächter, A., Biegler, L.T.: Line search filter methods for nonlinear programming: local convergence. SIAM J. Optim. **16**(1), 32–48 (2005)
18. Wächter, A., Biegler, L.T.: Line search filter methods for nonlinear programming: motivation and global convergence. SIAM J. Optim. **16**(1), 1–31 (2005)
19. Wächter, A., Biegler, L.T.: On the implementation of a primal-dual interior point filter line search algorithm for large-scale nonlinear programming. Math. Program. **106**(1), 25–57 (2006)
20. Yao, D.: A fractional dashpot for nonlinear viscoelastic fluids. J. Rheol. **62**(2), 619–629 (2018)